Numerical Analysis on Connection Problem of a Fiber to an Embedded Waveguide with Rectangular Cross-section Using Fourier Series Expansion Method*

Michiko MOMODA**, Tokuo MIYAMOTO** and Kiyotoshi YASUMOTO***

An effective numerical method, Fourier series expansion method, is presented for connection problem between two three-dimensional optical waveguide systems. As the numerical example, we try more accurate full-wave analysis on connection problem of a step-index optical fiber to an inhomogeneous embedded optical waveguide whose relative permittivity distribution in the rectangular cross section is parabolic. Then the effects of the gap and the transverse shifts between both waveguides are made clear, comparing with the case of homogeneous embedded optical waveguide. It is also confirmed that this method is effective for more accurate full-wave analysis of various kinds of three-dimensional waveguide systems constructed by arbitrarily shaped waveguides with arbitrary medium.

Key Words: Optical Fiber, Embedded Thin-Film Waveguide, Parabolic Index Profile, Connection Problem, Full-Wave Analysis

1 Introduction

Practical optical waveguide system is usually constructed by complicated three-dimensional waveguide, then reflected and radiation fields must be taken into consideration. Moreover, in the cases where the waveguide has large transverse refractive index difference (Δn) or mode conversion occurs, full-vectorial analysis is needed, and rigorous analysis on such waveguide system is important for precise designing of various optical devices. However, it seems very difficult to practice rigorously full-vectorial analysis on complicated three-dimensional waveguide system including large Δn. Many approaches have been attempted so far. For examples, the waveguide systems with tapers, branches and directional couplers and also the discontinuity problems, using finite-difference time-domain (FDTD) method[1] and beam propagation method improved so as to include reflection field (BPM)[(2)~(4)] and so on. As for the problems including reflection field, three-dimensional waveguide system has been analyzed by Vassalo[5], but they are not full-vectorial analysis and limited in the case of smaller Δn. Kendall et al.[6] have tried full-vectorial analysis for connection problem of two waveguides using free space radiation method. However it is not effective for the waveguide including the larger transverse index variation of the structure composed of three layers, such as, film, substrate and cover (air) in usual thin-film optical waveguide. Pregla et al.[7] also proposed full-vectorial analysis for three-dimensional periodic waveguide using MOL-BPM, but actually they calculated two-dimensional case. On the other hand, although the reflection is not treated, vectorial analysis for uniform waveguide has been reported by Kendall et al.[8], Rahmann et al.[9] and Marcuse[10]. They have used **E** or **H** vector wave equation, then the solutions obtained by each equation are not always coincident.

Generally speaking, numerical approach on full-vectorial treatment of three-dimensional complicated waveguide system including the case of large Δn needs large computational memory and time, and many researchers have developed various

* 平成15年11月30日受付
** Department of Electronics Engineering and Computer Science, Faculty of Engineering, Fukuoka University
*** Faculty of Information Science and Engineering, Kyushu University

approaches to reduce computational effort. However, because of rapid progress of computer technology in these days, such a computational effort does not seem to be so severe. Then, putting emphasis on accuracy, conveniency and simplicity of the algorithm, we have proposed a full-vectorial straightforward method, Fourier series expansion method, for three-dimensional complicated waveguide system in which Maxwell equations are solved directly instead of wave equations.

The basis of the method has been proposed by Rokushima et al.[11),(12] for diffraction problem, and Hosono et al.[13] Yamakita et al.[14] and Yasumoto et al.[15),(16] mainly in the two-dimensional waveguide system by scalar analysis. Recently, we have extended it to full-vectorial analysis of various kinds of three-dimensional waveguide systems[17]~(29). In this method, virtual periodicity in both transverse directions is introduced into the waveguide structure, and the original waveguide is approximated by one period of the waveguide arrays. Under assumed periodic condition, Maxwell's equations are discretized directly. That is, both electric and magnetic fields which satisfy Maxwell's equation are expanded in double Fourier series using the complex trigonometric functions. Then the problem is reduced to a simple eignvalue one of a set of linear equations for the Fourier coefficients in which any transverse derivatives of permittivity of the medium is not included, and the whole fields can be obtained simultaneously by solving one fundamental equation. Those features mentioned above are said to be advantages of the proposed method. Thus the solutions yield the full-vectorial fields for the guided and discretized radiation modes, propagating both in forward and backward directions along the waveguide even in the case of large Δn. The accuracy of the solution can be improved by increasing the truncation number of the Fourier expansions, although the computational cost increases. Numerical method using Fourier series expansion has been also reported by Henry et al.[30] for scalar wave equation, and Marcuse[10] (already cited above) for vector wave equations. However they solve wave equation, then the solution obtained by wave equation on the electric field is not always same with that obtained by wave equation on the magnetic field[10].

Using the Fourier series expansion method, we have analyzed a step discontinuity problem in three-dimensional waveguide systems with inhomogeneous core, using the proposed full-vectorial method[21),(25)~(29]. This time we analyzes the connection problem of a step-index optical fiber (radius $r=3\lambda$, 4λ, refractive index difference $\Delta n=0.3\%$, 1.0%) to an embedded thin-film optical waveguide ($\Delta n=0.6\%$, 1.0%) with inhomogeneous relative permittivity distribution in the rectangular cross-section ($8\lambda\times4\lambda$)[26),(27]. Then the effects of the gap and the transverse shifts of the center axes between two waveguides are made clear, comparing with the case of homogeneous permittivity distribution.

2　Formulation of the problem

As the three dimensional waveguide system, we consider Fig.1. That is, a dominant mode is incident from a step-index optical fiber (region Ⅰ) to a semi-infinite embedded thin-film optical waveguide with rectangular cross-section (region Ⅲ), through the gap (region Ⅱ). Then more accurate analysis is tried to the guided and radiation modes propagating both in forward and backward directions along the waveguides. In this paper we assume $\exp(j\omega t)$, and ω is angular frequency of the incident wave. In Fig. 1, ε_{f1} and ε_{c1} are relative permittivities of the core and cladding in optical fiber, respectively, ε_g is that of the gap region, and $\varepsilon_{f3}(x,y)$, ε_s and ε_{c3} are those of film, substrate and cover in region Ⅲ, respectively. For convenience, we normalize the coordinate variables by the wavenumber $k_0\,(=\omega\sqrt{\varepsilon_0\mu_0})$ in free space, the electric field by $(\varepsilon_0/\mu_0)^{1/4}$, and the magnetic field by $(\mu_0/\varepsilon_0)^{1/4}$, where ε_0 and μ_0 are permittivity and permeability in free space, respectively. Then the normalized electric and magnetic fields satisfy the Maxwell's equations:

$$\nabla\times\mathbf{E}(x,y,z)=-j\mathbf{H}(x,y,z),$$
$$\nabla\times\mathbf{H}(x,y,z)=j\varepsilon(x,y)\mathbf{E}(x,y,z) \qquad (1)$$

where $\varepsilon(x,y)$ includes the whole relative permittivities in the cross section concerned.

3　Numerical method

More detailed algorithm of the method is explained in the literatures[19),(29].

To solve eq.1 in each region, we introduce an

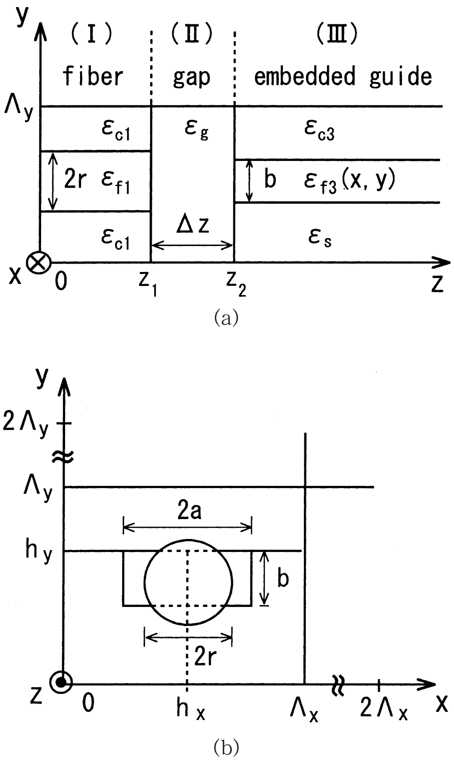

Fig.1 (a) Side view of the waveguides system and (b) cross-sectional view of the first period of the assumed periodic waveguide array

artificial periodic structure with the periods Λ_x and Λ_y in the x and y directions, respectively, and approximate the original waveguide structure in terms of one period of the periodic arrays as shown in Fig.1(b). For the assumed structure, $E_i(x, y, z)$ and $H_i(x, y, z)\,(i = x, y, z)$ are approximated by the truncated double Fourier series expansion as follows

$$E_i(x, y, z) = \sum_{m=-M}^{M} \sum_{n=-N}^{N} e^i_{m,n}(z)\exp(-jsmx)\exp(-jtny),$$

$$H_i(x, y, z) = \sum_{m=-M}^{M} \sum_{n=-N}^{N} h^i_{m,n}(z)\exp(-jsmx)\exp(-jtny),$$

$$i = x, y, z, \quad s = 2\pi/\Lambda_x, \quad t = 2\pi/\Lambda_y \tag{2}$$

Equation 2 is substituted into eq.1. The resulting equations are multiplied by $\exp(jsm'x)\exp(jtn'y)/(\Lambda_x\Lambda_y)$ and integrated over $0 \le x \le \Lambda_x$ and $0 \le y \le \Lambda_y$. Using the orthogonality of the complex Fourier series, they are lead to a set of linear differential equations in matrix form for the expansion coefficients $\{e^i_{m,n}(z)\}$ and $\{h^i_{m,n}(z)\}\,(i = x, y)$:

$$d\mathbf{f}(z)/dz = -j\mathbf{C}\mathbf{f}(z) \tag{3}$$

Here, we introduce vectorial notations for the expansion coefficients as

$$\mathbf{e}^i(z) = [e^i_{-M,-N} \cdots e^i_{-M,N} \cdots e^i_{M,-N} \cdots e^i_{M,N}]^t,$$
$$\mathbf{h}^i(z) = [h^i_{-M,-N} \cdots h^i_{-M,N} \cdots h^i_{M,-N} \cdots h^i_{M,N}]^t, \ i = x, y$$
$$\mathbf{f}(z) = [\mathbf{e}^x(z)\ \ \mathbf{e}^y(z)\ \ \mathbf{h}^x(z)\ \ \mathbf{h}^y(z)]^t \tag{4}$$

and define the cyclic matrix $\mathbf{A}$ of order K ($K = (2M+1)(2N+1)$) which consists of the double Fourier components of $\varepsilon(x, y)$ as

$$\mathbf{A} = [\varepsilon_{p,q}], \tag{5}$$

$$\varepsilon_{p,q} = \frac{1}{\Lambda_x\Lambda_y}\int_0^{\Lambda_x} dx \int_0^{\Lambda_y} dy\ \varepsilon(x, y)\exp(-jspx) \cdot\exp(-jtqy) \qquad p = m - m',\ q = n - n' \tag{6}$$

and the superscript "t" in eq.4 indicates transpose of vectors. Then $\mathbf{C}$ is expressed as

$$\mathbf{C} = \begin{bmatrix} \mathbf{0} & \mathbf{0} & \mathbf{MA}^{-1}\mathbf{N} & -\mathbf{MA}^{-1}\mathbf{M} + \mathbf{I} \\ \mathbf{0} & \mathbf{0} & \mathbf{NA}^{-1}\mathbf{N} - \mathbf{I} & -\mathbf{NA}^{-1}\mathbf{M} \\ -\mathbf{NM} & \mathbf{M}^2 - \mathbf{A} & \mathbf{0} & \mathbf{0} \\ -\mathbf{N}^2 + \mathbf{A} & \mathbf{NM} & \mathbf{0} & \mathbf{0} \end{bmatrix} \tag{7}$$

of order 4K, where $\mathbf{0}$ and $\mathbf{I}$ are the null and unit matrices of order K. The diagonal matrices $\mathbf{M}$ and $\mathbf{N}$ of order K are defined by

$$\mathbf{M} = [sm\,\delta_{mm'}\delta_{nn'}], \ \mathbf{N} = [tn\,\delta_{mm'}\delta_{nn'}] \tag{8}$$

where $\delta_{mm'}$ is the Kroneker's delta.

Thus the problem of the mode propagation in each region is reduced to an eigenvalue problem of the matrix $\mathbf{C}$, and we can utilize the standard calculational subroutine. The order of obtained eigenvalues $\kappa_k\,(k = 1, 2, \cdots\cdots, 4K)$ is generally unrelated to the order of actual eigenvalues of the waveguide. Then we rearrange the order of κ_k according to the magnitude of $|\kappa_k|$, after labeling the forward propagating modes as "+" and the backward one as "−". Thus the k-th mode satisfying $|\kappa_k| > \sqrt{\varepsilon_s}$ is the guided modes and the case $|\kappa_k| < \sqrt{\varepsilon_s}$ is the radiation modes. In the case where κ_k is imaginary, the field becomes evanescent wave. Here the eigenvalue κ_k for the radiation mode is obtained by discrete value because of the assumed periodic structure. From the rearranged eigenvalues $\pm\kappa_k$ $(= \beta_k/k_0)\,(k = 1, 2, \cdots, 2K)$ of matrix $\mathbf{C}$ and the associated eigenvectors $\mathbf{P}^{\pm}_k$, we can determine propagation constants $\pm\beta_k$, field distributions, and polarization states of both guided and radiation modes which are propagating in the $\pm z$ directions.

We introduce a new vectorial function $\mathbf{a}(z)$ of order 4K which satisfy

$$\mathbf{f}(z)=\mathbf{P}\mathbf{a}(z) \tag{9}$$

Here

$$\mathbf{P}=[\mathbf{P}^{+}\ \ \mathbf{P}^{-}],\ \mathbf{P}^{\pm}=[\mathbf{P}_1^{\pm}\ \ \mathbf{P}_2^{\pm}\ \ \cdots\cdots\mathbf{P}_{2K}^{\pm}],$$
$$\mathbf{a}(z)=[\mathbf{a}^{+}(z)\ \ \mathbf{a}^{-}(z)],\ \mathbf{a}^{\pm}(z)=[a_1^{\pm}\ \ a_2^{\pm}\ \ \cdots\cdots\ \ a_{2K}^{\pm}]^t \tag{10}$$

where $a_k^{\pm}$ is a complex mode amplitude for the k-th eigenmode, propagating along $\pm z$ directions. Then the solution of eq.3 is obtained as follows :

$$\mathbf{f}(z)=\mathbf{P}\begin{bmatrix}\exp[-j\kappa_k(z-z_0)]\delta_{kk'} & \mathbf{0}\\ \mathbf{0} & \exp[j\kappa_k(z-z_0)]\delta_{kk'}\end{bmatrix}\mathbf{a}(z_0) \tag{11}$$

Here the bracket [ ] indicates a diagonal matrix of order 4K and $\mathbf{a}(z_0)$ is the value of $\mathbf{a}(z)$ at $z=z_0$. Thus electric and magnetic fields can be obtained by substituting each component of eq.11 into eq.2 for each normalized propagation constant κ_k in the k-th mode. The eigen vector $\mathbf{P}_k$ is normalized so that the power carried by the respective k-th mode along z direction equals to $|a_k|^2$ [19].

4 Application to the connection problem

Now, we apply the method to the connection problem as shown in Fig.1. Expansion coefficients in vectorial form in each region are expressed as $\mathbf{f}^i(z)$ (i= Ⅰ, Ⅱ, Ⅲ) by eq.11, respectively. Similarly, complex amplitude vectors, eigenvalues and eignvectors are expressed as $\mathbf{a}^i(z)$, κ_k^i and $\mathbf{P}^i(z)$ (i= Ⅰ, Ⅱ, Ⅲ), respectively.

The boundary conditions for transverse electric and magnetic fields at $z=z_1$ and z_2 are satisfied by equating the respective Fourier coefficients in vectorial form for the fields in both sides of the boundaries as follows :

$$\mathbf{f}^{\mathrm{I}}(z_1)=\mathbf{f}^{\mathrm{II}}(z_1),\ \mathbf{f}^{\mathrm{II}}(z_2)=\mathbf{f}^{\mathrm{III}}(z_2) \tag{12}$$

They are lead to the following equation

$$\begin{bmatrix}\mathbf{a}^{\mathrm{III}+}(\mathbf{z}_2)\\ \mathbf{a}^{\mathrm{I}-}(0)\end{bmatrix}=[\mathbf{P}^{\mathrm{III}+}\ \ -\mathbf{A}_2]^{-1}[-\mathbf{P}^{\mathrm{III}+}\ \ \mathbf{A}_1]^{-1}\begin{bmatrix}\mathbf{a}^{\mathrm{III}-}(\mathbf{z}_2)\\ \mathbf{a}^{\mathrm{I}+}(0)\end{bmatrix} \tag{13}$$

where

$$[\mathbf{A}_1\ \ \mathbf{A}_2]=\mathbf{P}^{\mathrm{II}}\begin{bmatrix}\exp(-j\kappa_k^{\mathrm{II}}(z-z_1))\delta_{kk'} & \mathbf{0}\\ \mathbf{0} & \exp(j\kappa_k^{\mathrm{II}}(z-z_1))\delta_{kk'}\end{bmatrix}$$
$$(\mathbf{P}^{\mathrm{II}})^{-1}\mathbf{P}^{\mathrm{I}}\begin{bmatrix}\exp(-j\kappa_k^{\mathrm{I}}z_1)\delta_{kk'} & \mathbf{0}\\ \mathbf{0} & \exp(j\kappa_k^{\mathrm{I}}z_1)\delta_{kk'}\end{bmatrix} \tag{14}$$

As initial conditions, we consider the incidence of dominant mode $\mathrm{HE}_{11}^{\mathrm{I}}$ from optical fiber in region Ⅰ and no reflection in the region Ⅲ due to the assumption of semi-infinite waveguide. That is

$$\mathbf{a}^{\mathrm{I}+}(0)=[1\ \ 0\ \ \cdots\ \ 0]^t,\quad \mathbf{a}^{\mathrm{III}-}(z_2)=\mathbf{0} \tag{15}$$

Substituting eq.15 into eq.13, we obtain the solutions $\mathbf{a}^{\mathrm{III}+}(z_2)$ and $\mathbf{a}^{\mathrm{I}-}(0)$. From these solutions, we obtain the transmitted powers of guided and radiation modes as

$$T_g=\sum_{k=1}^{K_3}|a_k^{\mathrm{III}+}(z_2)|^2,\ T_r=\sum_{k=K_3+1}^{2K}|a_k^{\mathrm{III}+}(z_2)|^2 \tag{16}$$

respectively, and the reflected powers as

$$R_g=\sum_{k=1}^{K_1}|a_k^{\mathrm{I}-}(0)|^2,\ R_r=\sum_{k=K_1+1}^{2K}|a_k^{\mathrm{I}-}(0)|^2 \tag{17}$$

respectively, for each distance Δz of the gap (region Ⅱ) and transverse shifts along x and y directions of the center of the embedded waveguide. Here

$$T_g+T_r+R_g+R_r=1 \tag{18}$$

K_1 and K_3 are the numbers of guided modes in region Ⅰ and Ⅲ, respectively.

5 Numerical results

In the computation, the parameters in Fig.1 are chosen as $\sqrt{\varepsilon_{f1}}=1.5$, $\sqrt{\varepsilon_{c1}}=1.4955$ (refractive index difference $\Delta n=0.3\%$), 1.485 ($\Delta n=1.0\%$), $\sqrt{\Delta\varepsilon}=1.5-\sqrt{\varepsilon_s}$, $\sqrt{\varepsilon_s}=1.491$ ($\Delta n=0.6\%$), 1.485 ($\Delta n=1.0\%$), $\sqrt{\varepsilon_{c3}}=1.0$, $\sqrt{\varepsilon_g}=1.0, 1.5$, $r=3\lambda, 4\lambda$, $a=b=4\lambda$ and $\Lambda_x=\Lambda_y=30\lambda$. In this paper, circular core of optical fiber is approxi mated by rectangular arrays, and the convergency is shown in Fig.2 when the number of rectangular arrays L is increased. In practical computation we fix L as 100 which is seemed to be sufficient. In the case of inhomogeneous permittivity distribution in the rectangular cross section of the embedded waveguide, we assume parabolic profile as

$$\varepsilon_{f3}(x,y)=\Delta\varepsilon(1-(x-h_x)^2/a^2)(1-(h_y-y)^2/b^2)+\varepsilon_s \tag{19}$$

and in the case of homogeneous distribution as $\sqrt{\varepsilon_{f3}(x,y)}=1.5$.

The convergency of normalized propagation constants κ_1^{I} and κ_2^{III} in dominant modes $\mathrm{HE}_{11}^{\mathrm{I}}$ (E_y: dominant field) and $\mathrm{EH}_{11}^{\mathrm{III}}$ (E_y: dominant field) is shown in Fig.3(a),(b), respectively, when the truncation number M (=N) of the expansion in eq.2 increases. For smaller Δn, the convergency is faster. It is confirmed that the accuracy in the fiber is better than that in the embedded waveguide with rectangular cross-section. The convergency of the transmitted power T_{g2} of $\mathrm{EH}_{11}^{\mathrm{III}}$ mode is shown in Fig.3(c). It is confirmed that the accuracy of the field

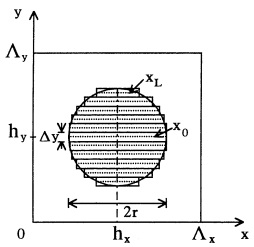

L	κ_1^{I}
10	1.496560173
30	1.496558002
40	1.496557687
50	1.496557500
60	1.496557155

Fig.2 Circular cross section of the step-index optical fiber approximated by rectangular arrays and convergency of normalized propagation constant κ_1^{I} when the number L of rectangular arrays increases, in the case of $r=3\lambda$, $\Delta n=1.0\%$, $M=N=10$

intencity becomes worse by about two or three figures than that of propagation constant. It is also confirmed that the convergency for κ_2^{III} in the case of homogeneous waveguide is faster than that of inhomogeneous waveguide (Fig.3(d)). In the following computations, we fixed M(=N) as 11, which seemed to be sufficient in order to explain the propagation characteristics of each waveguide system.

In Figs.4 and 5, it is confirmed that, for smaller Δn (solid curve), the field distributions become broader. It is noted that the peak point in the field distribution along y-axis of the embedded waveguide is more shifted toward the substrate, for the case of smaller Δn. This tendency is stronger in the case of inhomogeneous case. It is also confirmed that, in the case of inhomogeneous waveguide, the field distribution is more concentrated in the center than the case of homogeneous one.

From Figs.6(a)~6(c), it is confirmed that the transmitted power T_g decreases more slowly in the cases of $\sqrt{\varepsilon_g}=1.5$ (matching oil) and smaller Δn, when the gap distance Δz is increased largely (upper figure). In the case of $\sqrt{\varepsilon_g}=1.0$ (air gap), however, it should be noted that, because the gap region becomes a resonator, the transmitted power T_g becomes maximum when m is even number in $\Delta z=m\lambda/4$ and minimum when m is odd number, as shown in each lower figure for fine variation of Δz. Then, it is noted that the maximum power of the transmitted guided modes T_g decreases by about 15% due to the appearance of the reflected guided modes R_g in the case of the worst coupling in the air gap connection, while the transmitted radiation loss T_r is kept almost constant value ($R_r \sim 0$). It should be noted that transmitted loss T_r is smaller in the

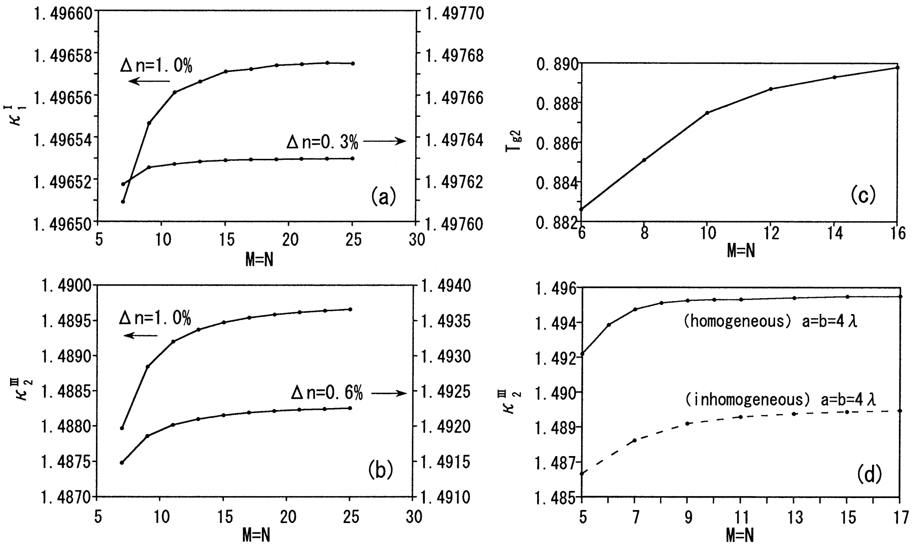

Fig.3 Convergencies of normalized propagation constants (a) κ_1^{I} of the dominant mode HE_{11}^{I} (E_y : dominant) in the optical fiber ($r=3\lambda$), (b) κ_2^{III} of EH_{11}^{III} (E_y: dominant) mode in the inhomogeneous embedded waveguide ($a=b=4\lambda$), (c) transmitted power $T_{g2}=|a_2^{\mathrm{III}}|^2$ and (d) comparison of the convergencies between the prapagation constants κ_2^{III} in the inhomogeneous and homogeneous waveguides ($a=b=4\lambda$, $\Delta n=1.0\%$) ($\Lambda_x=\Lambda_y=20\lambda$)

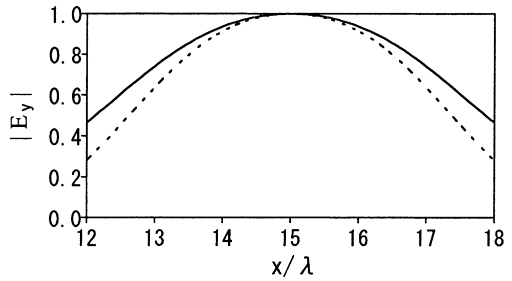

Fig.4 Field distributions of dominant mode HE^{I}_{11}(E_y: dominant) along x-axis in step-index optical fiber (r＝3λ) (——: Δn＝0.3%, ----: Δn＝1.0%)

case of smaller core radius of the fiber, then the transmitted guided power T_g becomes larger (compare Fig.6(a) with Fig.6(b),(c)). It is also noted that reflected guided power R_g is smaller and the variation of the transmitted guided power T_g for rough variation of Δz is slower in the case of smaller Δn in the out put waveguide (region Ⅲ) (compare Fig.6(b) with 6(c)).

Fig.7 shows the variations of each power when the center of the embedded waveguide is shifted along x- and y-axes of the cross section in the case of optimum gap distance. The transmitted power of the guided mode decreases by about 10% even when the waveguide center shifts only ±λ for Δn＝1.0%, while the decrease becomes more slowly for smaller Δn. In those inhomogeneous cases, the number of guided modes is 2, that is HE^{III}_{11}, EH^{III}_{11}, then the transmitted mode is only EH^{III}_{11} (E_x＝0, E_y is dominant) in the case of HE^{I}_{11} mode (E_y is dominant) incidence. It is also confirmed that, for smaller Δn, as the peak point of the field distribution along y-axis shifts toward the substrate of the inhomogeneous waveguide (refer Fig.5(a)), the peak point of the transmitted power shifts toward the substrate, keeping the peak power almost constant (upper figure in Fig.7(b)). It is noted that the peak value of T_g is larger in the case of smaller core radius of the fiber (compare (a) and (b)).

On the other hand, Fig.8 shows the homogeneous case, for comparison. In this case, although rectangular size is the same as that of inhomogeneous case, 4 guided modes for Δn＝0.3% (Fig.8(b)), and 8 guided modes for Δn＝1.0% (Fig.8(a)) can propagate. Then, as the transverse shift increases, higher order modes such as EH^{III}_{21} (for

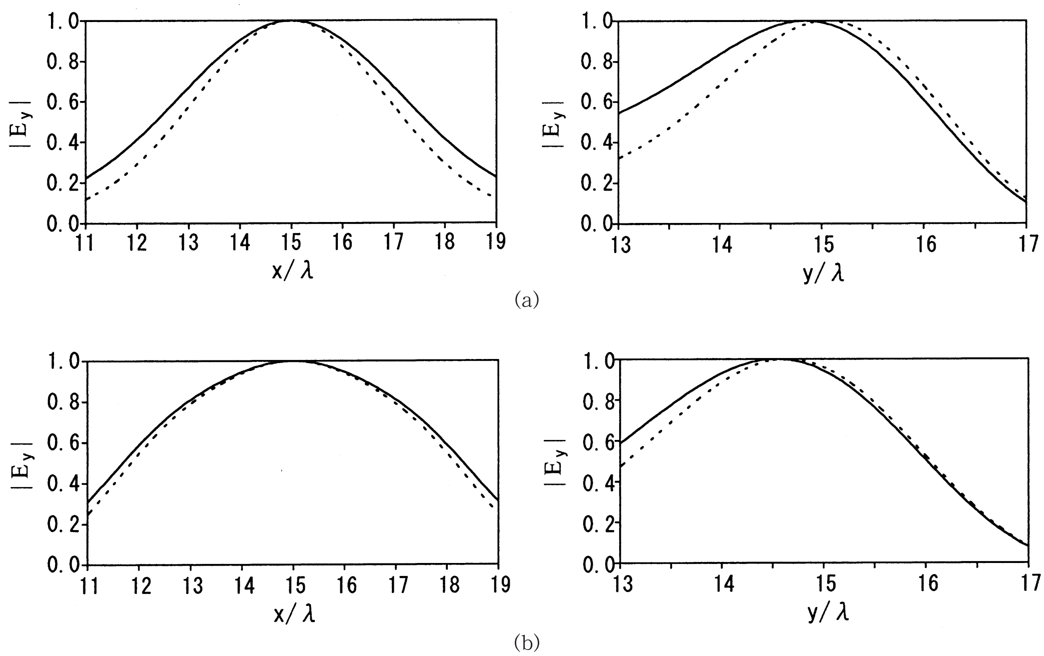

Fig.5 Field distributions of EH^{III}_{11} (E_y: dominant) along x- and y-axes in (a) inhomogeneous embedded waveguide, and (b) homogeneous embedded waveguide, a＝b＝4λ (——: Δn＝0.6%, ----: Δn ＝1.0%)

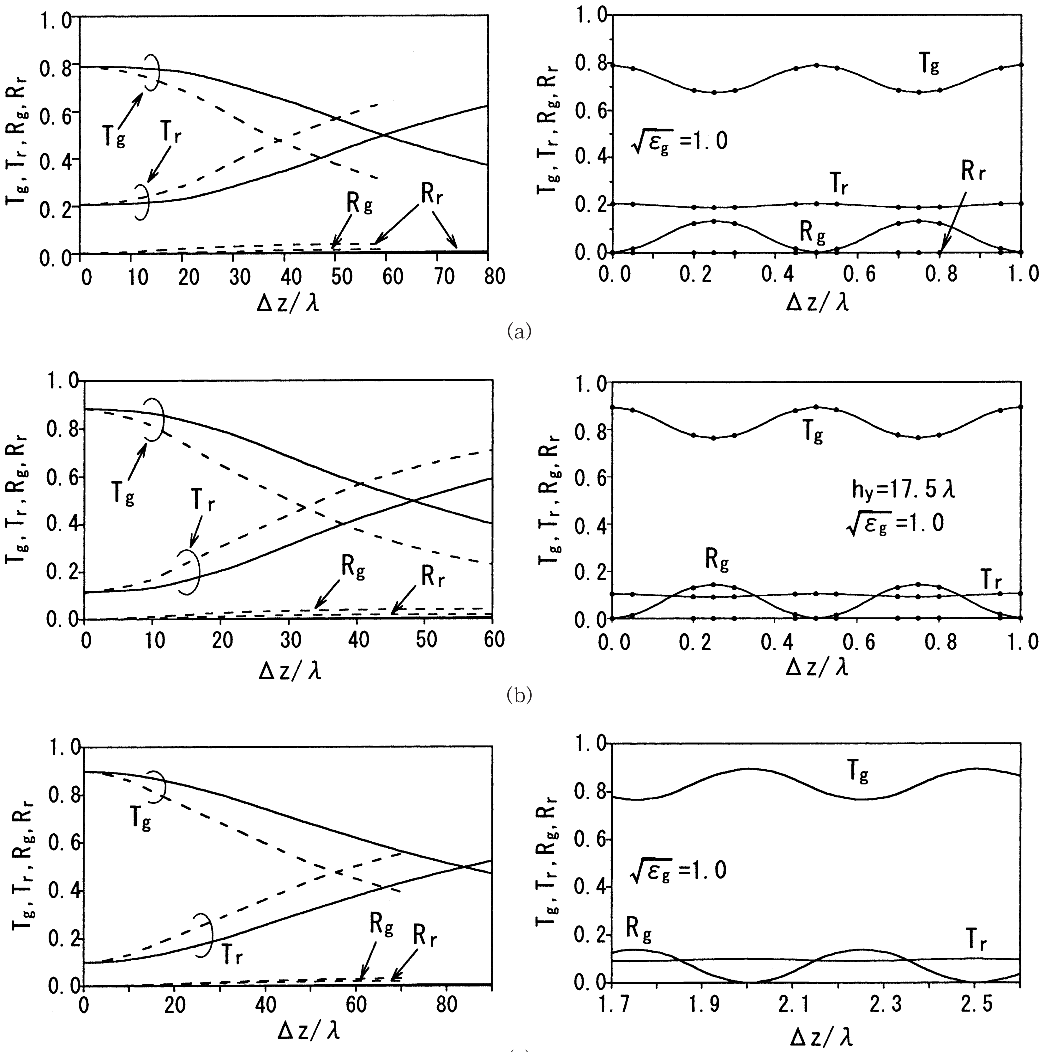

Fig.6 Variation of each power when the gap distance Δz between a step-index optical fiber and an inhomogeneous embedded optical waveguide is changed
{left figure : rough variation of Δz for $\sqrt{\varepsilon_g}=1.5$(solid line) and $\sqrt{\varepsilon_g}=1.0$(dashed line)
rigth figure : variation of the peak value of each power in the case of $\sqrt{\varepsilon_g}=1.0$ for fine variation of Δz
(a) $r=4\lambda$ ($\Delta n=1.0\%$), $a=b=4\lambda$ ($\Delta n=1.0\%$)
(b) $r=3\lambda$ ($\Delta n=1.0\%$), $a=b=4\lambda$ ($\Delta n=1.0\%$)
(c) $r=3\lambda$ ($\Delta n=0.3\%$), $a=b=4\lambda$ ($\Delta n=0.6\%$)

κ_4^{III}), EH_{31}^{III}(for κ_6^{III}) and EH_{12}^{III} (for κ_8^{III}) appear as shown in Fig.8. In this case, it is noted that modes (EH_{21}^{III}, EH_{31}^{III}, ……) whose field pattern varies along x-axis appear only in the shift along x-axis (lower figure in Fig.8(a)), but modes (EH_{12}^{III}, ……) whose field pattern varies along y-axis appear only in the shift along y-axis (upper figure in Fig.8(a)). Thus, as the shift becomes larger than only λ, the transmitted power of the unwanted higher order modes can not be negligible. It is noted that, in the homogeneous case, the transmitted radiation power T_r is larger (lowest figure in Fig.8(b)) comparing to the case of inhomogeneous case (Fig.6(c)) for the same values of Δn and sizes.

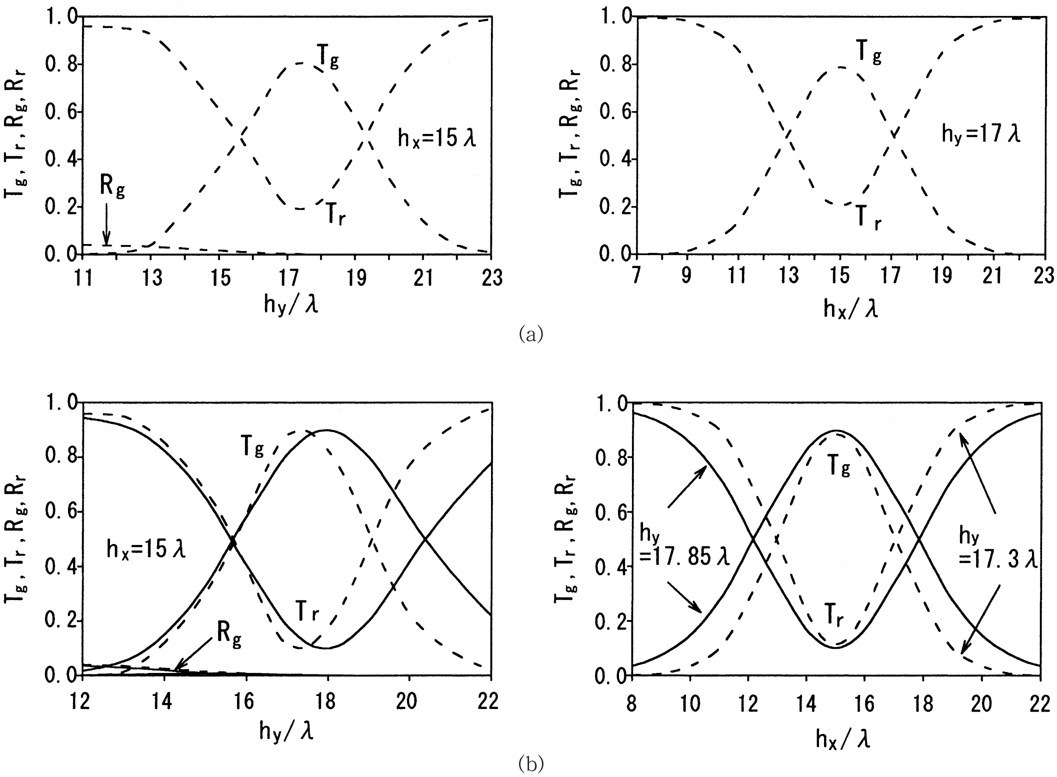

Fig.7 Variation of each power when the center of inhomogeneous embedded waveguides (number of guided modes : 2) is shifted along x- and y-axes ($\Delta z=2\lambda$, $R_g, R_r \sim 0$)
(a): r= a=b=4λ, (b): r=3λ, a=b=4λ
[—— : $\Delta n=0.3\%$ for fiber, $\Delta n=0.6\%$ for embedded waveguide
---- : $\Delta n=1.0\%$ for both waveguides]

Fig.9 shows the case of Ti : $LiNbO_3$ inhomogeneous embedded waveguide ($\sqrt{\varepsilon_{f3}}=2.23$, $\sqrt{\varepsilon_{c3}}=1.0$, $\sqrt{\varepsilon_s}=2.2077$) instead of glass waveguide ($\sqrt{\varepsilon_{f3}}=1.5$). It is noted that the magnitudes of T_r and the difference between maximum and minimum values in the oscillation of T_g and R_g for the variation of gap distance Δz become larger (Fig.9(b)) than the cases of glass waveguide (Fig.6) because of larger reflactive indices difference between $\sqrt{\varepsilon_c}$ and $\sqrt{\varepsilon_{f3}}$ ($\sqrt{\varepsilon_s}$). Then the variation of T_g due to the misalignment of Δz becomes larger, and the peak value of T_g becomes smaller than the cases of glass waveguide. However, it should be noted that the oscillation as a resonator of the gap almost vanishes for $\sqrt{\varepsilon_g}=\sqrt{1.5\times 2.23}=1.8289$ (dashed line), then the misalignment problem in the connection does not occur in this case, and the reflection R_g can also be neglected.

As conclusion, in the connection problem treated in this paper, in order to obtain larger transmitted power of single guided mode, inhomogeneous embedded waveguide with smaller Δn and fiber with smaller r are suitable. If the gap region is filled by matching medium, the oscillation of the T_g and R_g almost vanishes.

In results mentioned above, we chose the case where E_y is dominant field in HE_{11}^{I} mode in optical fiber, then the transmitted mode is almost restricted by EH_{11}^{III} mode whose dominant field is E_y. We also confirmed that, in the case where HE_{11}^{I} mode whose dominant field is E_x is incident, the transmitted mode is restricted by HE_{11}^{III} mode whose dominant field is E_x and the difference of the powers T_g and T_r between both cases is smaller than 0.5% (see

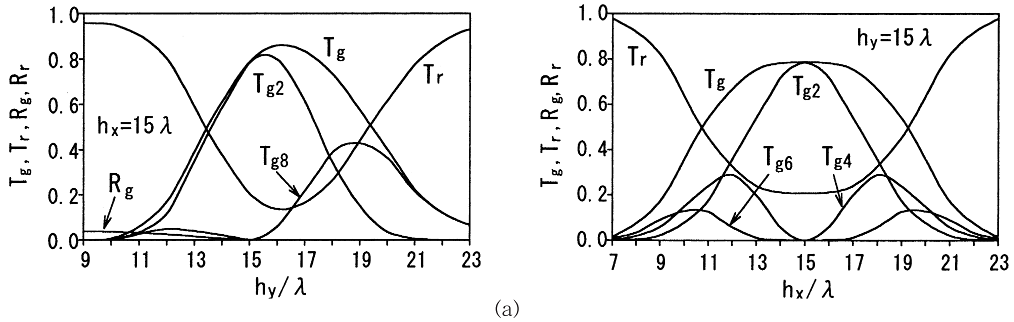

(a)

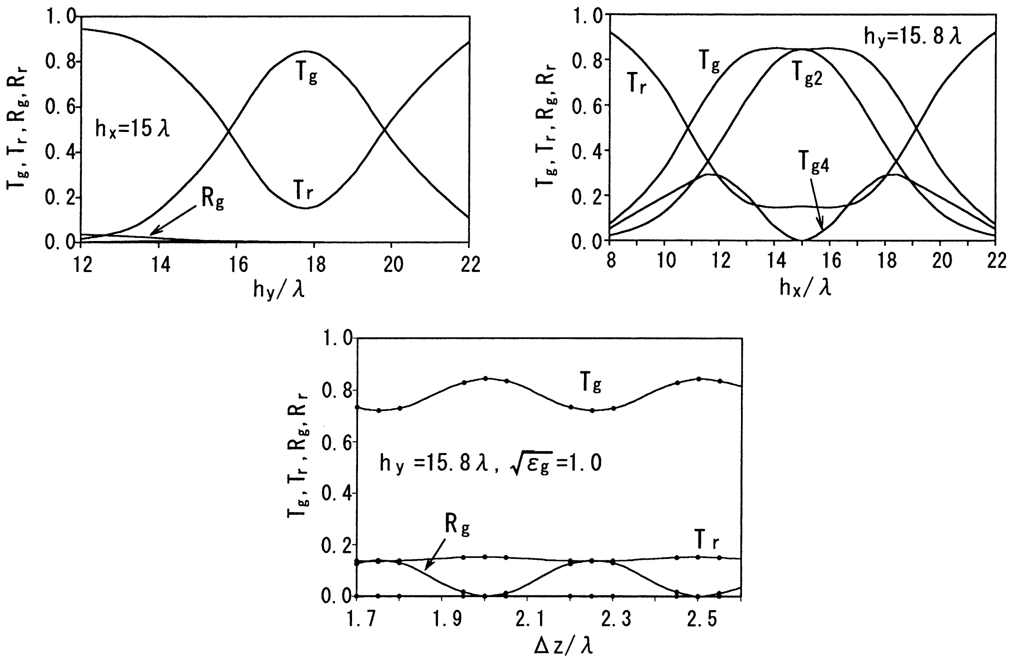

(b)

Fig.8 Variation of each power when the center of homogeneous embedded waveguide is shifted along x- and y-axes ($\Delta z=2\lambda$, $R_g, R_r<10^{-3}$)
(a) $r=4\lambda$ ($\Delta n=1.0\%$), $a=b=4\lambda$ ($\Delta n=1.0\%$ number of guided modes : 8)
(b) $r=3\lambda$ ($\Delta n=0.3\%$), $a=b=4\lambda$ ($\Delta n=0.6\%$ number of guided modes : 4)

$$\begin{bmatrix} T_{g2}=|a_2^{\text{III}}|^2 : EH_{11}^{\text{III}}, & T_{g4}=|a_4^{\text{III}}|^2 : EH_{21}^{\text{III}} \\ T_{g6}=|a_6^{\text{III}}|^2 : EH_{31}^{\text{III}}, & T_{g8}=|a_4^{\text{III}}|^2 : EH_{21}^{\text{III}} \end{bmatrix}$$

Table I) and R_g, R_r hold almost same value. In Table II, examples of computing time and memory in the present computer are listed.

6 Conclusion

Numerical method which uses the double Fourier series expansion and the virtual periodicity in both transverse directions is applied for more accurate and full-wave analysis on the connection problem of a step-index optical fiber to an inhomogeneous embedded thin-film optical waveguide. Then the propagation characteristics in the connection problem are made clear for a few refractive index differences of both waveguides,

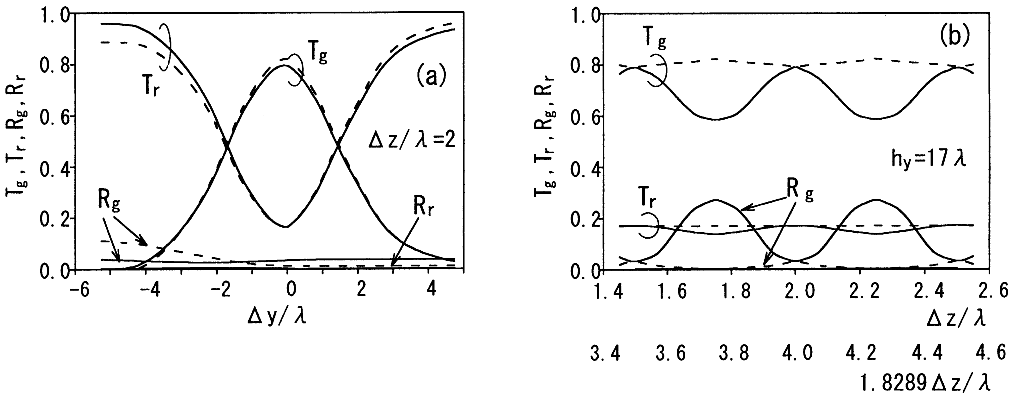

Fig.9 Variation of each power when (a) the gap Δz is changed and (b) the center of inhomogeneous Ti : $LiNbO_3$ embedded waveguide is shifted along y-axis
(――― : $\sqrt{\varepsilon_g}=1.0$, ---- : $\sqrt{\varepsilon_g}=1.8289$)
($r=3\lambda$, $a=b=4\lambda$, $\sqrt{\varepsilon_{f1}}=1.5$, $\sqrt{\varepsilon_{c1}}=1.485$, $\sqrt{\varepsilon_{f3}}=2.23$, $\sqrt{\varepsilon_{c3}}=1.0$, $\sqrt{\varepsilon_s}=2.2077$)

Table Ⅰ. Example of each output power when HE^{I}_{11} mode whose dominant field is E_y or E_x in the fiber is incident

	$h_y=15\lambda$		$h_y=17.5\lambda$ (center)	
input / output	$HE^{I}_{11}(E_y)$	$HE^{I}_{11}(E_x)$	$HE^{I}_{11}(E_y)$	$HE^{I}_{11}(E_x)$
T_g	0.2661	0.2748	0.7668	0.7725
T_r	0.6462	0.6375	0.0823	0.0959
R_g	0.0863	0.0861	0.1311	0.1311
R_r	0.0013	0.0014	0.0003	0.0003

$T_g=|a_1^{III+}(z_2)|^2(HE^{III}_{11})$ or $|a_2^{III+}(z_2)|^2(HE^{III}_{11})$
$R_g=|a_1^{I-}(0)|^2(HE^{I}_{11}(E_y))$ or $|a_2^{I-}(0)|^2(HE^{I}_{11}(E_x))$
$T_r=\sum_{k=K_3}^{2K}|a_k^{III+}(z_2)|^2$, $R_r=\sum_{k=K_1}^{2K}|a_k^{I-}(0)|^2$

Table Ⅱ. CPU time and memory (super computer FACOM VPP700/56)

eigenvalues of all modes for M=N=15	6 min.(240MB)
eigenvalues and eigenvectors of all modes for M=N=15	26 min.(352MB)
eigenvalues and eigenvectors of all modes for M=N=11	6 min.(136MB)
mode amplitudes and powers of all modes for M=N=15	79 min.(1168MB)
mode amplitudes and powers of all modes for M=N=11	20 min.(384MB)

comparing with the case of homogeneous permittivity distribution. It is also confirmed that this method is effective for more accurate full-wave analysis of three-dimensional waveguide system composed of arbitrarily shaped waveguides and complicated structure with arbitrary medium. In this method, saving of computational cost is also confirmed by using a differential equation of second order concerning electric or magnetic field, instead of eq.3, because the order of matrix **C** of eq.7 can be reduced to half [(19), (29)].

7 References

(1) W.P. Haung, S.T. Chu and S.K. Chaudhuri: ‘A semi-vectorial finite-difference time-domain method’, IEEE. Photon. Technol. Lett., Vol. 3, pp.803-806 (1991).
(2) M. Koshiba and Y. Tsuji : ‘A wide-angle finite element beam propagation method’, IEEE. Photon. Lett., Vol. 8, No. 9, pp.1208-1210 (1996).
(3) J. Shibayama, M. Sekiguchi, J. Yamauchi and H. Nakano: ‘Eigenmode analysis of optical waveguides by an improved finite-difference imaginary-distance beam propagation method’, Trans. Inst. Electr. Infor. Commun. Eng. JAPAN, Vol. J81-C-1, No.1, pp.9-16 (1998) (in Japanese).
(4) J. Yamauchi, G. Takahashi and H. Nakano: ‘Full-vectrial beam-propagation method based on the McKee-Mitchll scheme with improved finite-difference formulas’, J. Lightwave Technol., Vol. 16,

No. 12, pp.2458-2464 (1998).

(5) C. Vassalo : 'Theory of practical calculation of antireflection coating on semiconductor laser diode optical amplifiers' IEE Proc., Vol.137, pp.193-202 (1990).

(6) D.M. Read, P. Sewell, T.M. Benson and P.C. Kendall : 'Efficient propagation algorithm for 3D optical waveguides', IEE. Proc. optoelectron., Vol. 145, No. 1, pp.53-58 (1998).

(7) S. Helfert and R. Pregla : 'Efficient analysis of periodic structures', J. Lightwave Technol., Vol. 16, No. 9, pp.1694-1702 (1998).

(8) S. Sujecki, T.M. Benson, P. Sewell and P.C. Kendall : 'Novel vectorial analysis of optical waveguides', J. Lightwave Technol., Vol. 16, No.7, pp.1329-1335 (1998).

(9) S.S.A. Obayya, B.M.A. Rahman and H.A. El-Mikati : 'New full-vectorial numerically efficient propagation algorithm based on the finite element method', J. Lightwave Technol., Vol.18, No.3, pp. 409-415 (2000).

(10) D. Marcuse : 'Solution of the vector wave equation for general dielectric waveguide by Galerkin method', IEEE. J.Quantum Electr., Vol.28, No.2, pp.459-465 (1992).

(11) K. Rokushima and J. Yamakita : 'Analysis of anisotropic dielectric gratings', J. Opt. Soc. Am., Vol. 73, No. 7, pp.901-908 (1983.7).

(12) S. Mori, K. Mukai, J. Yamakita and K. Rokushima : 'Analysis of dielectric lamellar gratings coated with anisotoropic layers', J. Opt. Soc. Am., Vol.77, No.9, pp.1661-1665(1990.9).

(13) T. Hosono, T. Hinata, and A. Inoue : 'Numerical analysis of the discontinuities in slab dielectric waveguides', Radio Science, Vol. 17, No. 1, pp.75-83 (1982).

(14) J. Yamakita, K. Matsumoto and K. Rokushima : 'Analysis of discontinuities in anisotoropic dielectric waveguides', IEICE Technical Report, EMT-93-87, pp.81-89 (1993) (in Japanese).

(15) K. Yasumoto, H. Maeda and S. Morita : 'Numerical analysis of transition and discontinuities in optical waveguides', Asia-Pacific microwave conference Proc., Delhi, pp.647-650 (1996).

(16) K. Yasumoto and K. Ohzawa : 'Analysis of a step transition in optical fibers using periodic boundary conditions', Asia-Pacific microwave conference Proc., Hong Kong, pp.665-668 (1997).

(17) T. Miyamoto, M. Momoda and K. Yasumoto : 'Analysis of an embedded dielectric waveguide with parabolic index distribution in the two-dimensional cross section', 1998 Int. Conf. on Microwave and Millimeter wave Technology Proc., Beijing, pp.841-844 (1998).

(18) M. Momoda, T. Miyamoto and K. Yasumoto : 'Numerical analysis of a two-parallel dielectric waveguide with parabolic index profile', Proc. of 1998 China-Japan joint meeting on Microwaves, Beijing, pp.82-85 (1998).

(19) T. Miyamoto, M. Momoda and K. Yasumoto : 'Numerical analysis of three-dimensional optical waveguide using Fourier series expansion method', Fukuoka University Review of Thechnological Sciences, Vol. 64, pp.167-185 (2000. 3) (in Japanese).

(20) M. Momoda, T. Miyamoto and K. Yasumoto : 'Full-vectorial analysis on field distribution of higher-order mode (EH_{11}) in optical fiber', Technical Report of IEICE, OPE2000-89, pp.53-58 (2000.11) (in Japanese).

(21) T. Miyamoto, M. Momoda and K. Yasumoto : 'Mechanism of higher-order mode occurrence due to the shift of center axis in the connection of optical fibers', The paper of Technical Meeting on Electromagnetic Theory, IEE Japan, EMT-00-106, pp.43-48 (2000.10) (in Japanese).

(22) T. Miyamoto, M. Momoda and K. Yasumoto : 'Full-vectorial analysis of optical directional coupler', 2000 Japan-China Joint Meeting on Optical Fiber Science and Electromagnetic Theory, pp.231-234, Osaka, Japan (2000.12).

(23) T. Miyamoto, M. Momoda and K. Yasumoto : 'Full-vectorial Fourier modal analysis of three-dimensional optical waveguide', Proc. of Progress In Electromagnetics Research Symposium, p.103, Osaka, Japan (2001.7).

(24) M. Momoda, T. Miyamoto and K. Yasumoto : 'Full-vectorial analysis for field distribution of eigenmodes in optical fiber using Fourier series expansion method', Fukuoka University Review of Thechnological Sciences, Vol. 68, pp.49-62 (2002.3) (in Japanese).

(25) T. Miyamoto, M. Momoda and K. Yasumoto : 'Investigation of higher-order mode occurrence

due to the shift of center axis of two optical fibers', Fukuoka University Review of Thechnological Sciences, Vol. 68, pp.63-70 (2002.3) (in Japanese).

(26) M. Momoda, T. Miyamoto and K. Yasumoto : 'Analysis on connection problem of three- dimensional optical waveguide using Fourier series expansion method', Technical Report of IEICE, OPE98-98, pp.55-60 (1998.11) (in Japanese).

(27) M. Momoda, T. Miyamoto and K. Yasumoto : 'Analysis on connection problem of three-dimensional optical waveguide using Fourier series expansion method (Ⅱ)' , Technical Report of IEICE, EMT-99-65, pp.65-71 (1999.8) (in Japanese).

(28) M. Momoda, T. Miyamoto and K. Yasumoto : 'Numerical analysis on connection problem in embedded thin-film optical waveguide', Fukuoka University Review of Thechnological Sciences, Vol. 64, pp.75-102 (2000.3) (in Japanese).

(29) T. Miyamoto, M. Momoda and K. Yasumoto : 'Full-vectorial analysis of connection problem in optical fiber', Trans. IEE of Japan, Vol. 122-A, No. 1, pp.39-46 (2002.1).

(30) C. Henry and Y. Shami : 'Analysis of mode propagation in optical waveguide devices by Fourier expansion", IEEE J. Quantum Electr., Vol. 27, No.3, pp.523-530 (1991).